Fabrication 3d Tissue Engineering Scaffold Poly(Ethylene) Diacrylate Filled with Aramid Nanofiber: Mechanical Evaluation and Toxicity

A. Nurulhuda, S. Izman, Nor Hasrul Akhmal Ngadiman

Abstract: The selection of the optimum scaffold fabrication method becomes challenging due to a variety of manufacturing methods, existing biomaterials and technical requirements. Although, Digital light processing (DLP) 3D printing process is one of the SLA techniques which commonly used to fabricate tissue engineering scaffold, however, there is no report published on the fabrication of tissue engineering scaffold-based PEGDA filled with Aramid Nanofiber (ANFs). Hence, the feasible parameter setting for fabricating this material using DLP technique is currently unknown. This work aims to establish the feasible setting parameter via DLP 3D printing to fabricate PEGDA/ANFs 3D tissue engineering scaffold. Preliminary study has been done to identify the accurate composition and curing time setting in producing scaffold. In this work, the researcher has proved the potential and capability of these novel composition biomaterial PEGDA/ANFs to be print via DLP-3D printing technique to form a 3D structure which is not yet been established and has not reported elsewhere.

Keywords : Biomaterials, 3D Printing, Tissue Engineering, Scaffold, Additive Manufacturing

I. INTRODUCTION

This failure of organs or tissues due to trauma or ageing is a primary concern in healthcare as they are costly and devastating problems. This has led to the development of tissue engineering (TE), which aims to create biological substitutes to repair or replace the failing organs and tissues [1]. One of the best approaches in tissue engineering is growing biodegradable scaffold cells, which it attempts to imitate the natural extracellular matrix function and provide a temporary tissue growth template [2]. Tissue engineering scaffolds are unique in a way; they are able to establish three-dimensional environments for propagated cells and provides specific recognition molecules which capable of mimicking the environment of natural tissues. The scaffolds can be either natural, synthetic or hybrid. [3].

A. Nurulhuda, Quality Engineering, Universiti Kuala Lumpur (UniKL), Johor, Malaysia [1] School of Mechanical Engineering, Universiti Teknologi Malaysia (UTM), Johor, Malaysia [2]
S. Izman, School of Mechanical Engineering, Universiti Teknologi Malaysia (UTM), Johor, Malaysia[2]
Nor Hasrul Akhmal Ngadiman*, School of Mechanical Engineering, Universiti Teknologi Malaysia (UTM), Johor, Malaysia. [2]

A useful tissue engineering scaffold should fulfil the biological and mechanical target tissue requirements. The scaffolds should have an appropriate microstructure to support cell proliferation, contained with open-porous geometry with a highly porous surface enabling cell growth, appropriate surface morphology and a predictable degradation rate of non-toxic material [4].

Tissue regeneration in scaffolds through cell implantation relies primarily on the scaffold structure and the nature of the biomaterials [5]. When selecting the right material for scaffolds, the interaction between biomaterials and surrounding tissues is a crucial concern. Although the particular material demands rely on the nature of the implementation, the biocompatibility of all biomaterials must be assessed [6]. The biomaterial scaffolds will allow cells to generate and activate molecules as a transplant, enabling the regeneration of functional tissue in the host as an alternative to prevalent organ transplantation and tissue reconstruction practices [3]. Essentially, an optimal biomaterial scaffold could mimic the natural structure and process of bone tissue regeneration by varying the biomolecules that give almost equal to mechanical strength for cell seeding and sufficient interconnected open porosity which is comparable to natural bone [7].

Nanoscale fibrous structures have gained much interest in tissue engineering field application. Nanofiber has emerged as promising biomimetic candidates of scaffold due to their large surface to volume ratio [8]. The high surface-to-volume ratio of nanofibers for tissue engineering applications is extremely desired. This nano-environment allows for cells grow and it has the potential to optimize cell adherence, proliferation, migration and cell differentiation, which similar to natural extracellular matrices (ECM) of tissues and organs [9]. Therefore, nanofiber systems have been strongly pursued as scaffolds for tissue engineering applications.

Poly(ethylene glycol) diacrylate (PEGDA) hydrogel polymer has been found extensively in biomedicine compare to other hydrogel biopolymers due to their excellent performance in biocompatibility and hydrophilicity [10]–[12]. Even though various PEGDA-based scaffolds were reported; however, none of them fulfils all the requirements for tissue engineering applications [13]. These materials exhibit poor mechanical properties because of their poor physical and mechanical stability [14], [15].

Retrieval Number: L29161081219/2019©BEIESP
DOI: 10.35940/ijitee.K2916.1081219
Journal Website: www.ijitee.org

1997

Published By:
Blue Eyes Intelligence Engineering
& Sciences Publication

Fabrication 3d Tissue Engineering Scaffold Poly(Ethylene) Diacrylate Filled with Aramid Nanofiber: Mechanical Evaluation and Toxicity

Besides, PEGDA hydrogel is also lacking cell adhesion, limiting its use as tissue engineering scaffold [16]. To overcome these limitations, some researchers added hydrogels polymers with nanofiller such as carbon nanotube (CNT), nano-silica, laponite nanoparticle, and so on [17]–[19].

It has been proven that nano environments capable to enhance cell adhesion, cell proliferation, and mechanical properties of tissue engineering scaffold [9]. Although a lot of work has been reported, there is unreported work done on PEGDA hydrogels filled with ANFs specifically in tissue engineering scaffold applications. Previous studies only discussed issues related to kinetic crystallization and morphology of PEGDA hydrogel with Kevlar fibers at the macro scale. There is no literature provides detailed information on the structural and mechanical properties of PEGDA filled with Aramid nanofibers (ANFs).

In the current situation, the most common nanofillers used in tissue engineering are bioceramic, bioglass, and carbon nanotube [20]. Unfortunately, these fillers have several limitations. For example, bioceramic and bioglass nanofillers appear to have brittle properties, fragile and low fracture strength compared to natural bone, unsuitable for load-bearing scaffolding [21]. These materials are also challenging to fabricate due to poor flexibility properties. Low fatigue strength behavior also makes them incompatible with being used in the formulation of tissue engineering hydrogels [22]. The use of carbon nanotube (CNTs) as filler in tissue engineering scaffold is minimal due to lack in biodegradability. CNTs are nonbiodegradable and may remain in an organism as reported by researchers [23], [24], who observed the CNTs depositing at the cell's nucleus and migration in extracellular locations. Similar results were reported by Mu *et al*. (2009), and Liu *et al*. (2010), where a high concentration of CNT contributed to negative effect for cell proliferation [23]–[26]. On the other hand, one of obvious limitation of CNTs application in tissue engineering is their high stiffness properties, which never be able to mimic the mechanical properties of tissues and considered to be critical for the proliferation of cell [27].

Even though there are numerous types of potential materials that can be used as tissue engineering scaffolds, however, aramid fibers are considered as a high-performance organic material with special characteristics to be used in scaffold fabrication. Aramid nanofiber offers excellence in mechanical properties, good acid and alkali resistance, excellent dielectric, good thermal and chemical resistance, and relatively favorable hydrophilicity [28], [29]. In 2002, Jassal and Gosh were reported that the first organic fiber with high enough tensile modulus and tensile strength to be used as reinforcement in advanced composite was an aromatic polyamide fiber or aramid fiber. It is exhibited by 5% to 10% higher mechanical properties compared than other synthetic fibers [30]. Aramid fiber are light (density = 1.44g/cm^3), strong (tensile strength = 3.6GPa), resist to impact and damage [29], [31]. Aramid fiber composite usually used for the reason of their high tensile strength, rigidity, fatigue resistance, and stress rupture is essential. Additionally, aramid nanofiber can also be achieved easily by dissolving commercial Kevlar (para-aramide) fiber in suitable organic solutions. It is appropriate for large production and development of high-performanc ultrafiltration membranes [32].

Aramid (known as Kevlar) is the generic name for aromatic polyamide fibers [33]. Kevlar is a well-known macroscale synthetic para-aramid fiber with a high tensile strength-to-weight ratio. Typical Kevlar threads and fibers consist of lengthy molecular chains made of poly (paraphenylene terephthalamide) (PPTA) between which there are interchain bonds making the material highly strong and rigid with a tensile strength of 3.6GPa and modulus comparable as carbon nanotube (CNT) fibers [34], [35]. By dissolving in dimethylsulfoxide (DMSO), aramid macroscale fibers can be divided into nanofibers in the presence of potassium hydroxide (KOH) [35].

In 2008, researchers conducted an investigation into aramid fiber bio-conformity compared to frequently used polyester fibers with known biological impacts. Results of investigation demonstrated that aramid fibers cause minimal tissue reaction, which caused primarily in cell growth and differentiation (cytokinins). Other than that, aramid fibers also exhibited higher static and dynamic mechanical strength compared to polyester fibers. Besides, they did not bio-corrode and could be used to increase the mechanical strength of medical material or like independent bio-material under high mechanical loads [36]. Chuanxiong *et al.* (2017) reported the use of aramid nanofiber (ANF) to enhance the ultrafiltration and biological performances of polysulfone (PSf) and polyethersulfone (PES) membranes. Aramid nanofibers (ANF) were used in biomedical applications to enhance blood compatibility specifically in protein adsorption, suppressed platelet adhesion and activation, inhibited coagulant variables and supplementary activation variables [37]. However, the use of PEGDA/ANFs as a tissue engineering scaffold has not been reported elsewhere, and their mechanical and biodegradable properties remain unknown.

Therefore, the present work in this research study is aim to close the gap by synthesized a new biomaterial-based on Poly (ethylene glycol) diacrylate (PEGDA) filled with Aramid nanofiber (ANF) for tissue engineering scaffold application. The feasible DLP 3D printing parameters in producing high strength scaffold with biocompatible properties were analyzed in detail.

II. METHODOLOGY

A. Materials

Chemicals used in this study were as follows: 1) Potassium hydroxide (KOH) (90% purity, Sigma Aldrich), 2) Dimethyl sulfoxide (DMSO) (QRёC), 3) Kevlar (160 mg), 4) Poly (ethylene glycol) diacrylate (PEGDA) (Mn 700, Sigma Aldrich) and 5) 2,4,6-trimethylbenzoyl-diphenylphosphine oxide (TPO) (97% purity,

Sigma Aldrich), and Dulbecco's modified essential medium (DMEM).

B. Synthesis of ANFs

In order to prepare the photopolymer solution, PEGDA (Mn 700) was dissolved in Dimethyl sulfoxide (DMSO) to obtain a solution with concentrations of 30% wt. Aramid Nanofiber (ANFs) has been synthesized based on the method reported by Guan et. al., (2017). The solution was then magnetically stirred continuously for 1 week at room temperature until a dark red ANF/DMSO dispersion (2.0 mg/ml) obtained.

Fig. 1 shows steps involved to split bulk Kevlar fibers into aramid nanofibers by deprotonation (removal a hydrogen cation, H+) in the solution of DMSO and KOH. The ANFs solution was dried under room environment in order to allow the formation of a thin sheet of ANFs. The diameter of the single dried nanofiber was observed under the Field Emission Scanning Electron microscope.
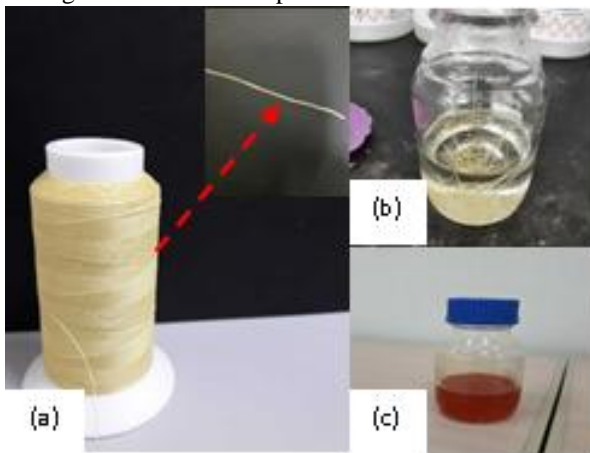
Fig. 1. (a) Bulk Kevlar, (b) Kelvar dissolved in DMSO and KOH, (c) orange coloured of ANF dispersion after stirred one week at room temperature.

C. Digital Light Processing Setup (DLP) Machine

The fabrication of 3D tissue engineering scaffolds was carried out using commercially available DLP 3D printing machine (FEMTO 3D) with resolution up to 23 µm. Fig. 2 shows the set-up of this machine. DLP machine uses digital projector to cure layer by layer of photosensitive resin. A very thin slice of the 2D layer is created with each pass of the laser. The process is repeated again and again until the part is completed. The laser hardens (cures) the resin by forming a solid layer. During the process of DLP 3D printing, the UV beam traces a 2D cross-section onto a base submerged in a tank of liquid photoactive resin that polymerizes upon illumination. After completion of 2D cross-section, the UV beam begins the addition of the next layer, which is polymerized on top of the previous layer. In between layers, a blade loaded with resin levels the surface of the resin to ensure a uniform layer of liquid prior to another round of UV light exposure. This process is repeated, slice by slice until the 3D object is completed [20].
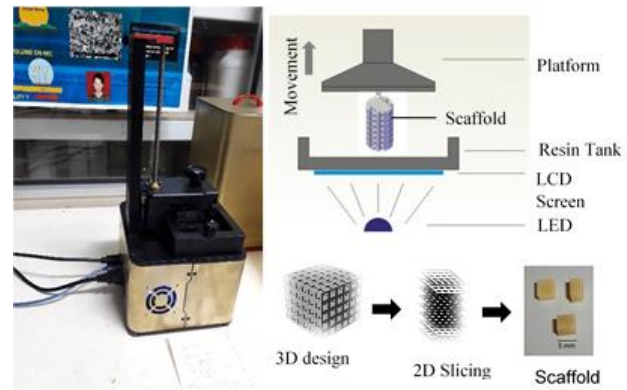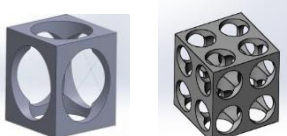

Fig. 2: Schematic diagram of DLP 3D printing process

SolidWorks 3D V14 software was used to model the scaffold structure design with a constant porosity value, cell size and number of unit cells based on the previous literature as summarized in Table 1. SolidWorks design file was converted into STL format for printing purpose. DLP printing process of the scaffold was conducted with curing time setting at 70 and 80s for different TPO concentrations. The printing layer thickness was fixed at 100 µm during printing. At the end of the printing process, the un-polymerized liquid resin was removed by post-curing within 24 hours to converts any unreacted groups of polymerization resin.

TABLE 1. Unit size of design scaffold [19]

Parameters (enclosed volume = 1000mm^3)		
Lattice Name	Single lattice	Lattices with 8 of unit
Cell Size (l/d=1.25)	l=10, d=8	
Total number of a unit cell	8	
Porous scaffold volume (mm^3)	1728.82	
Porosity (%)	79	

D. Calibration 3D Printing Process

In this research study, the composition ratio for PEGDA and photoinitiator to ANFs started at 1:9 and 9:1. The concentration of photoinitiator Diphenyl(2,4,6-trimethylbenzoyl)phosphine oxide (TPO) use was varied with the aims to initiate the crosslinking process of photopolymerization under DLP 3D printing. Calibration curing time printing was set started from 20s up to 180s. Result of calibration printing will observe in detail to get the accurate dimension of the 3D profile, as shown in Fig. 3.

The aims of the calibration printing process is to get feasible curing time setting which will be used directly during DLP printing for 3D structure scaffold. This is because the different varying ratio and concentration have their specific setting time.

Fabrication 3d Tissue Engineering Scaffold Poly(Ethylene) Diacrylate Filled with Aramid Nanofiber: Mechanical Evaluation and Toxicity

The process of a preliminary study in our research starts with setting time for the combination of PEGDA and TPO as a photoinitiator. The repeated experiment for curing time study was repeated for other composition ratio of resin: ANFs. The best setting of curing time will be used to print 3D design structure of scaffold
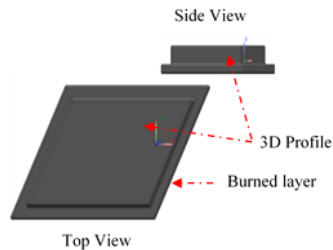

Fig. 3. Image of calibration printing 3D profile

E. Photoinitiator Concentration

In order to identify the effect of photoinitiator concentration on 3D profile formation, an experiment has been conducted by varying the concentration of TPO at 0.5, 1.0 and 1.7 %wt. The ratio of resin PEGDA: TPO (8:2) and resin to ANFs (9:1) are fixed. Result of the printed profile was recorded.

F. Mechanical Testing

All compression tests were performed perpendicular to the plane of the scaffold. The 3D scaffold PEGDA/ANFs was designed in a cylindrical shape (diameter: 0.5 inches; height: 4mm) according to ASTM standard D695 and printed by DLP 3D printing. Compression test was performed using Shimadzu Machine at testing speed 1 mm/min at room temperature. At least three samples measurement were performed to confirm the reproducibility of data. Stress-strain curves of the printed scaffold were plotted. Young's modulus value was obtained by fitting a line against a linear region of the data [38]. The stress-strain curves were plotted, and Young's modulus value was obtained by fitting a line against a linear region of the data [39], [40].

G. In Vitro Biocompatibility Study

Cytocompatibility study of PEGDA/ANFs scaffold was evaluated as described by the standard ISO10993-5, Biological evaluation of medical devices —Part 5: Tests for in vitro cytotoxicity. 1x105 cells were seeded in 96 well plates overnight and cultured till 80% confluence. The scaffold sample was prepared (1 cm diameter x 0.5 mm thickness). The PEGDA/ANFs scaffold samples were sterilized under ultraviolet (UV) condition. The hydrogel extract was diluted with DMEM, and samples were incubated for 24 h. After the incubation period, the solutions in the wells were discarded and replaced with fresh medium. 20 mL of MTT reagent in PBS was subsequently added to each well, and the plates were gently shaken and then incubated for 4 hours at 37 °C in 5% CO_2. Following incubation, the supernatant containing medium was aspirated, and 200 mL of DMSO was added to each well for 30 min under shaking at 80 rpm to solubilize the existing formazan complex. The absorbance of solubilized formazan product (dark purple) was then measured at 570 nm using commercial machine ELISA microplate reader.

III. RESULTS AND DISCUSSIONS

A. Microstructure Analysis ANFs

ANFs in solution phase was dried in ambient for 7 days to get a nanofiber mat. Fig. 4 shows the microstructure observation of dried ANFs with the smallest diameter size was recorded at range ~50 nm and the largest size at range ~ 80 nm. The microstructure result revealed that Kevlar fibers used in this research were successfully split into ANFs by concept of deprotonation.
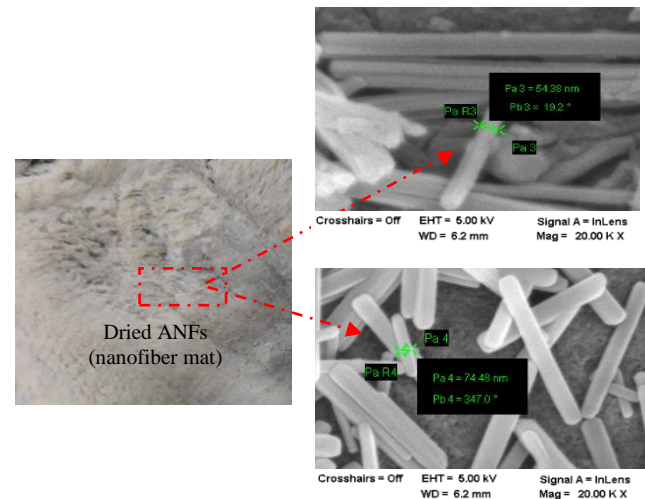

Fig. 4: FESEM image of a single diameter dried ANFs in nano-scale size.

The finding from our research also proved that ANFs was successfully mixed with PEGDA biopolymer without any coagulation happened (Fig. 5) and the resin formulation of PEGDA/ANFs biomaterials was proved capable to be print under a simple and low-cost method via DLP 3D printing process. This is because a homogeneous dispersion of filler is crucial in polymer nanocomposites. Agglomeration may occur in poorly dispersed nanofiller creating micron-sized aggregates. The previous study revealed that moderate interaction between filler and polymer creates optimum dispersion of filler. At low interaction, filler tends to attract each other, producing agglomerates while strong interaction between polymer and filler creating flocculates due to strong polymer adsorption to its neighboring filler [23].
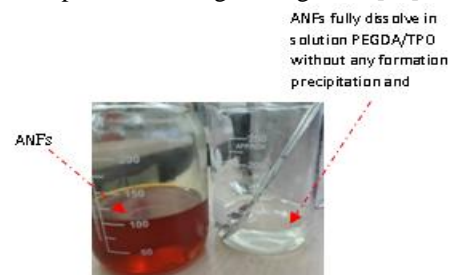

Fig. 5: ANFs completely dissolved in resin (PEGDA/TPO) without any coagulation formation.

The real development of nanoscale reinforcements become more challenging in real development the difficulties come from exfoliation and dispersion of existing materials. This is due to dissimilar chemical nature between nanofillers, and polymeric resin materials were said as the main reason for imperfect filler dispersion, which contributed to the low mechanical performance of composites relative to theoretical predictions. But, the result obtains from this research study shown that the PEGDA/ANFs biomaterial produced was found to be a more economical and most convenient way to enhance the mechanical properties of pure PEGDA biopolymer resin for the purpose as 3D tissue engineering scaffold application. The composition ratio formulation proposed in this research also contributed excellence result in producing new biomaterial resin without any imperfect filler dispersion condition.

B. Effect Concentration Photoinitiator on DLP 3D Printed Profile Formation

The results effect of photoinitiator concentration on 3D profile formation were recorded as in Fig. 6.

Referring to the result, it was observed that high concentration TPO (1.7 %wt.) was caused by the formation of a thin layer printed profile. The thin layer formation of the 3D profile is due to localization of high free radical initiation closer to the surface which caused the penetration depth of the photons laser decreased then produced in a tightly cross-linked and thin cured profile [23], [24]. The result of a repeated experiment at constant value ratio of % wt. PEGDA, TPO and ANFs with lower concentration TPO; 0.5 %wt. and 1 %wt. shown a clear and thick-3D profile cure formed is actually desirable at a lower initiator concentration 0.5% wt.

However, the dimension accuracy of the printed profile for 0.5 % wt was formed non-uniform and not consistence between each profile. On the other hands, higher curing time setting for 0.5 % wt TPO was also observed to cause inaccurate dimension (Fig. 5). Therefore, 1.0 %wt concentration of TPO is said to have much accurate dimension of printed profile compare than 0.5 %wt. Based on these finding, in order to confirm % composition of TPO to form a perfect 3D sample, the samples were print out with accurate dimension size as tensile test sample (ISO 37:2011). Both composition of TPO at 0.5 %wt. and 0.1 %wt. for constant ratio PEGDA: TPO (8:2) and resin: ANFs (9:1) were print at 70s of curing time. The printed results were recorded and analyzed, as shown in Table 2.

In Table 2, the most exceptional and accurate dimension of printed 3D tensile sample was recorded by 1.0 %wt. of TPO compare than the concentration at 0.5 %wt. The sample for 0.5 % wt. of TPO was not able to print within 70s and also at 80s of curing time which the sample formed in the semi-solid phase and not fully cured. This finding is aligned with collected data results in Fig. 6, which the 0.5% wt. concentration was produced non-uniform thickness profile. Hence, it can be concluded that 0.5% wt. concentration is actually will not able to perform a perfect of 3D sample for tensile test in real. The reason of thick-section cured is often desirable due to a lower initiator concentration [23]. Therefore, the researcher decides to print the final 3D pores scaffold structure PEGDA/ANFs by using photoinitiator TPO at 1.0 %wt. due to its ability to form the most accurate dimension of the 3D profile.
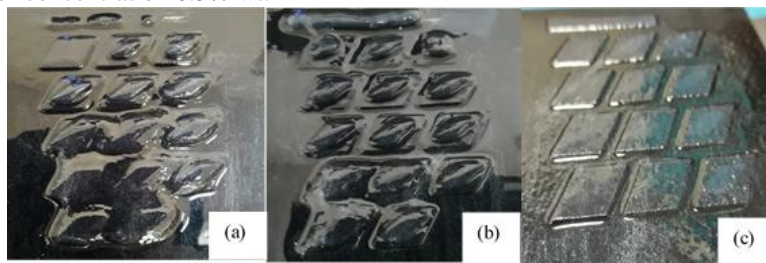

Fig. 6. Calibration printing profile resin: ANFs at constant 30% wt PEGDA with varied concentration of TPO; (a) 0.5 %wt, (b) 1.0 %wt and (c) 1.7 %wt

TABLE 2. 3D test sample print by DLP 3D printing with different concentration of %wt. of TPO

Composition/Concentration		Result	
PEGDA	TPO	Curing Time (s)	
30% wt	0.5 % wt	70	
30% wt	0.5 % wt	80	
30% wt	1 % wt	70	
30% wt	1 % wt	80	

C. Printable Formulation for PEGDA/ANFs 3D Tissue Engineering Scaffold

In order to access the capability and potential of PEGDA/ANFs to be print under DLP 3D printing, the 3D scaffold with the porous interior design was printed by referring to our preliminary setting with composition resin to ANFs at ratio 9:1 and 1.0 % wt. of TPO photoinitiator. Feasible curing time printing was decided at 70s due to the result obtained in Table 2.

The scaffold structure was observed in detail and measured. Fig. 7 show the result of 3D printed scaffold with pores. The novel biomaterial of PEGDA filled with ANFs was successfully, and capable to print via DLP technique with precise pore size and dimensional accuracy After post curing within 10h, the sample of scaffold structure were observed become stiffer due to complete photopolymerization under post-curing process.
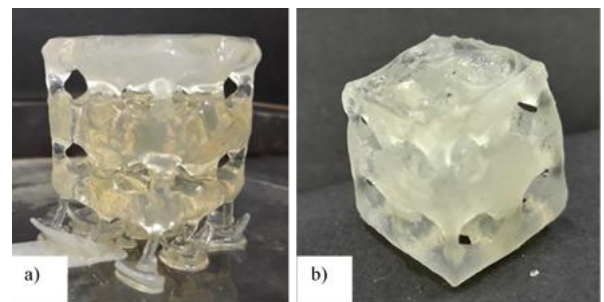

Fig. 7: 3D tissue engineering scaffold PEGDA/ANFs with porous structure; (a) before post-curing (b) after post-curing.

D. Mechanical Properties PEGDA/ANFs Tissue Engineering Scaffold

The compression test was performed to evaluate the mechanical properties of printed PEGDA/ANFs 3D scaffold. The mechanical value result will determine the strength of the scaffold. The Young's modulus value was recorded and obtained from Stress-strain curved plotted as in Fig. 8 (A-B). Based on the result, PEGDA/ANFs scaffold for ratio composition 9:1 was performed their strength value up to 0.10 MPa compare than pure PEGDA scaffold which shows only 0.05 MPa. The ANFs have simultaneously improved the stiffness and toughness of the polymer. It was found to be an efficient way to enhance the mechanical properties of polymeric composites.
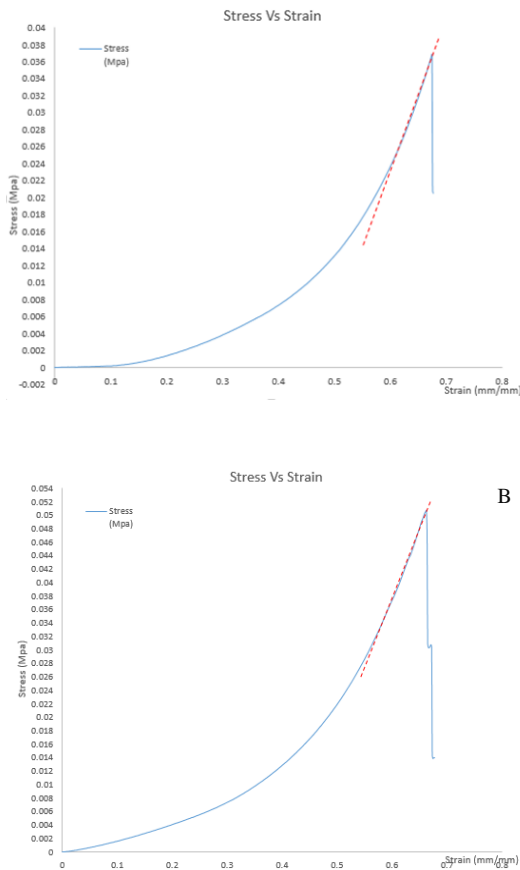

Fig. 8: Young's modulus plotted graph of the printed scaffold; (A) Pure PEGDA scaffold, (B) PEGDA/ANFs at ratio 9:1.

E. Biocompatibility Properties of PEGDA/ANFs Tissue Engineering Scaffold

The extent of cytotoxicity from every composition resin to ANFs was quantified and recorded in Table 3. By referring to ISO 10993-5, percentages of cell viability above 80% are considered as non-toxic within 80%–60% weak; 60%–40% moderate and below 40% strong cytotoxicity respectively [41], [42].

In this research study, the biocompatibility study of variable composition ratio PEGDA to ANFs at 7:3, 8:2 and 9:1 has been analyzed by MTT assay. As indicated in Fig. 9, the evaluation from composition resin formulation of
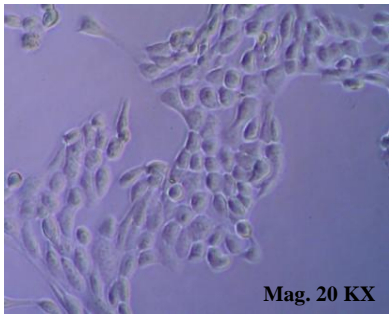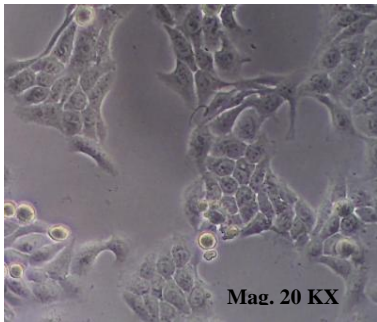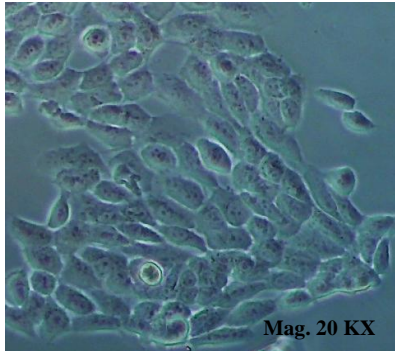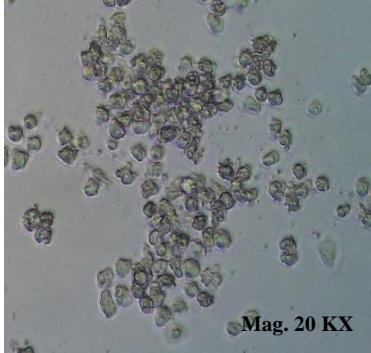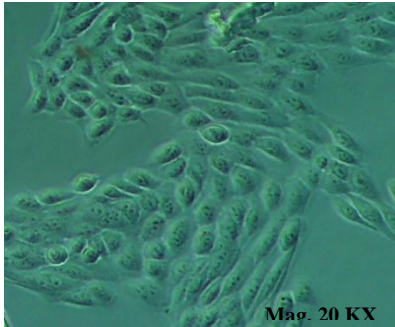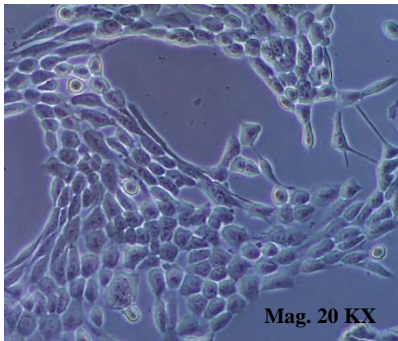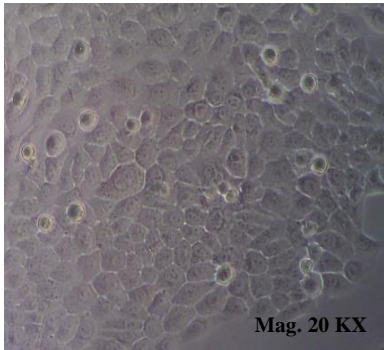
PEGDA/aramid scaffold, ratio resin to ANFs at 7:3 and 8:2 had low toxicity with high percentage cell's viability recorded at 106.6281% and 72.3386 % compared to concentration at 9:1 (62.81851 %). The finding in this research also demonstrates the excellent cytocompatibility of the Kevlar fiber, with well-stained cells growing all in the scaffold test sample for ratio 7: 3 compared than others ratio (Table 4). The result our research study in term of the cytotoxic effect of Kevlar proved to be consistent in the previous research which showed Kevlar to be very stable in the biological environment and to demonstrate excellent biocompatibility in vitro [43].

TABLE 3. Result of Cell Viability (%) Under MTT Assay Testing

	Control	7:3	8:2	9:1
	99.41379	124.4255	59.45756	66.89855
	102.6653	72.08848	88.15851	67.46131
	97.35032	121.0489	80.84258	52.20416
	102.4152	118.8604	82.53087	72.15101
	102.2276	83.59387	77.15335	67.46131
	97.28779	124.2379	44.95076	55.26809
	100.852	71.2756	90.09692	66.14819
	97.78803	137.4941	55.51821	54.95545
	100	106.6281	72.3386	62.81851
Average Std. dev.	2.186278	24.77528	15.66824	6.977116

Retrieval Number: L29161081219/2019©BEIESP
DOI: 10.35940/ijitee.K2916.1081219
Journal Website: www.ijitee.org

2003

Published By:
Blue Eyes Intelligence Engineering
& Sciences Publication

Fabrication 3d Tissue Engineering Scaffold Poly(Ethylene) Diacrylate Filled with Aramid Nanofiber: Mechanical Evaluation and Toxicity

TABLE 4. Result of Cell Viability after 24 hour

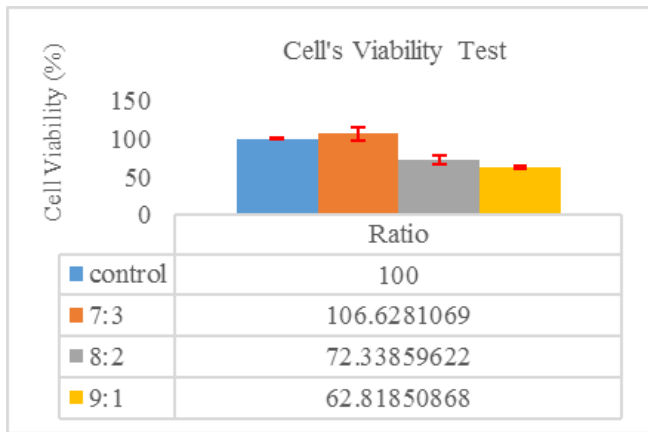| Condition	0 Hour	After 24 Hour
Control	Mag. 20 KX	Mag. 20 KX
9:1	Mag. 20 KX	Mag. 20 KX
8:2	Mag. 20 KX	Mag. 20 KX
7:3	Mag. 20 KX	Mag. 20 KX

Fig.9: Cytotoxicity at the different printable composition ratio of PEGDA/ANFs.
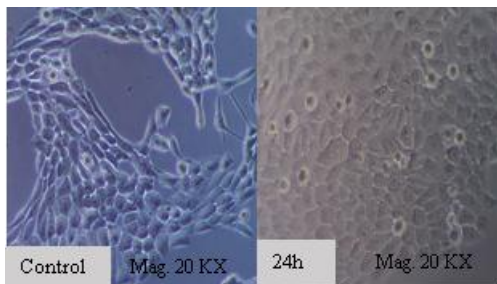

Fig. 10: High ratio ANFs (7:3) in PEGDA scaffold indicates increment in cell proliferation and increased overall cell viability (106.6281 %).

The HACAT cells in MTT assay were observed proliferate well in the presence of ANFs at 7:3 which high ratio ANFs in PEGDA scaffold indicated increment in cell proliferation and increased overall cell viability at 106.6281 % (Fig. 10). However, the cell did not proliferate very well in the ratio 8:2 with the cell's viability only at 72.3386 %. The MTT assay detects the purple formazan produced by mitochondrial enzymes, which are only present in metabolically active live cells. Therefore, the determination of live cell numbers was able to show the cell proliferation and cytotoxicity effect caused by cytotoxic agents. The result of more than 100 % viability cells showed the sample of PEGDA/ANFs was affect the mitochondrial activity of the cell. The increment in cell's viability with high printable composition ratio resin to ANFs up to 7:3 aligned with previous research which declared that the nano environment enhanced the cell adhesion and increased proliferation cells [9]. The cytotoxic analysis study in this researched confirmed that the PEGDA/ANFs is relatively safe for healthy cells, as agreed with the previous toxicity studies on the use of aramid fiber.

IV. CONCLUSION

In the present work, it can be concluded that the fabrication of a novel 3D tissue engineering scaffold of PEGDA filled with ANFs with a perfect profile formation, dimension and pores was successfully printed. The use of photoinitiator TPO was identified able to initiate the novel bioresin material of PEGDA with ANFs under DLP with wavelength ~405 nm. The Young's modulus value of PEGDA/ ANFs (9:1) printed scaffold recorded is at 0.10 MPa while pure PEGDA scaffold only shows 0.05 MPa. The used of ANFs was identify simultaneously improved the stiffness and toughness of the scaffold. In term of biocompatibility study, MTT assay showed week condition of the cell's viability at ratio 8:2 (72.3386 %). However, increased the composition ANFs was enhanced the cell proliferation and increased overall cell viability at 106.6281 %. The cytotoxic analysis study was confirmed that the PEGDA/ANFs tissue engineering scaffold is relatively safe for healthy cells.

REFERENCES

1. K. F. Leong, C. K. Chua, N. Sudarmadji, and W. Y. Yeong, "Engineering functionally graded tissue engineering scaffolds," J. Mech. Behav. Biomed. Mater., vol. 1, no. 2, pp. 140–152, 2008.
2. R. J. Mondschein, A. Kanitkar, C. B. Williams, S. S. Verbridge, and T. E. Long, "Polymer structure-property requirements for stereolithographic 3D printing of soft tissue engineering scaffolds," Biomaterials, vol. 140, pp. 170–188, 2017.
3. Chen, S. Liang, and G. A. Thouas, "Elastomeric biomaterials for tissue engineering," Prog. Polym. Sci., vol. 38, no. 3–4, pp. 584–671, 2013.
4. W.-Y. Yeong, C.-K. Chua, K.-F. Leong, and M. Chandrasekaran, "Rapid prototyping in tissue engineering: challenges and potential," Trends Biotechnol., vol. 22, no. 12, pp. 643–652, 2004.
5. M. Bil, J. Ryszkowska, and K. J. Kurzydłowski, "Effect of polyurethane composition and the fabrication process on scaffold properties," J. Mater. Sci., vol. 44, no. 6, pp. 1469–1476, 2009.
6. M. Bil, J. Ryszkowska, P. Woźniak, K. J. Kurzydłowski, and M. Lewandowska-Szumieł, "Optimization of the structure of polyurethanes for bone tissue engineering applications," Acta Biomater., vol. 6, no. 7, pp. 2501–2510, 2010.
7. J. Lim, M. You, J. Li, and Z. Li, "Emerging bone tissue engineering via Polyhydroxyalkanoate (PHA)-based scaffolds," Mater. Sci. Eng. C, vol. 79, pp. 917–929, 2017.
8. S. Ramakrishna, K. Fujihara, W. . Teo, T. Yong, Z. Ma, and R. Ramaseshan, "Electrospun nanofibers: Solving global issues," Mater. Today, vol. 9, no. 3, pp. 40–50, 2006.
9. R. Vasita and D. S. Katti, "Nanofibers and their applications in tissue engineering," Int. J. Nanomedicine, vol. 1, no. 1, pp. 15–30, 2006.
10. C.-W. Chang, A. Spreeuwel, C. Zhang, and S. Varghese, "PEG/clay nanocomposite hydrogel: a mechanically robust tissue engineering scaffold," Soft Matter, vol. 6, no. 20, p. 5157, 2010.
11. Cheung, K. T. Lau, T. P. Lu, and D. Hui, "A critical review on polymer-based bio-engineered materials for scaffold development," Compos. Part B Eng., vol. 38, no. 3, pp. 291–300, 2007.
12. H. Chen, L. Yuan, W. Song, Z. Wu, and D. Li, "Biocompatible polymer materials: Role of protein-surface interactions," Progress in Polymer Science, vol. 33, no. 11. pp. 1059–1087, 2008.
13. H. Kotturi et al., "Evaluation of Polyethylene Glycol Diacrylate-Polycaprolactone Scaffolds for Tissue Engineering Applications," J. Funct. Biomater., vol. 8, no. 3, p. 39, 2017.
14. P. K. Dutta, K. Rinki, and J. Dutta, "Chitosan: A promising biomaterial for tissue engineering scaffolds," Adv. Polym. Sci., vol. 244, no. 1, pp. 45–80, 2011.
15. B. Mahanta and R. Nigam, "An Overview of Various Biomimetic Scaffolds: Challenges and Applications in Tissue Engineering," J. Tissue Sci. Eng., vol. 05, no. 02, pp. 1–5, 2014.
16. G. Turnbull et al., "3D bioactive composite scaffolds for bone tissue engineering," Bioact. Mater., vol. 3, no. 3, pp. 278–314, 2018.

Retrieval Number: L29161081219/2019©BEIESP
DOI: 10.35940/ijitee.K2916.1081219
Journal Website: www.ijitee.org

2005

Published By:
Blue Eyes Intelligence Engineering
& Sciences Publication

17. Vashist, A. Kaushik, A. Ghosal, J. Bala, and R. Nikkhah-moshaie, "Nanocomposite Hydrogels : Advances in Nanofillers Used for Nanomedicine," Gels, vol. 4, no. 3, p. 75, 2018.

18. S. Mishra, F. J. Scarano, and P. Calvert, "Rapid prototyping of three-dimensional nanocomposite hydrogel constructs : Effect of silica nanofiller on swelling and solute release behaviors of the nanocomposite hydrogels," J. Biomed. Mater. Res., vol. 103, no. 10, pp. 3237–3249, 2015.

19. Chang, "PEG / clay nanocomposite hydrogel : A mechanically robust tissue engineering scaffold PEG / clay nanocomposite hydrogel : a mechanically robust tissue engineering scaffold," Soft Matter, no. 20, pp. 5157–5164, 2010.

20. G. Tozzi, A. De Mori, A. Oliveira, and M. Roldo, "Composite hydrogels for bone regeneration," Materials (Basel)., vol. 9, no. 4, pp. 1–24, 2016.

21. K. P. Saffar, N. Jamilpour, and G. Rouhi, "Carbon Nanotubes in Bone Tissue Engineering," Tissue Eng., no. October, pp. 477–498, 2008.

22. Brien and J. Fergal, "Biomaterials & scaffolds for tissue engineering," Mater. Today, vol. 14, no. 3, pp. 88–95, 2011.

23. E. Mooney, P. Dockery, U. Greiser, M. Murphy, and V. Barron, "Carbon nanotubes and mesenchymal stem cells: Biocompatibility, proliferation and differentiation," Nano Lett., 2008.

24. H. Haniu et al., "Basic potential of carbon nanotubes in tissue engineering applications," Journal of Nanomaterials. 2012.

25. D. Liu, C. Yi, D. Zhang, J. Zhang, and M. Yang, "Inhibition of proliferation and differentiation of mesenchymal stem cells by carboxylated carbon nanotubes," ACS Nano, 2010.

26. Q. Mu, G. Du, T. Chen, B. Zhang, and B. Yan, "Suppression of human bone morphogenetic protein signaling by carboxylated single-walled carbon nanotubes," ACS Nano, 2009.

27. P. L. H. Newman, "Carbon Nanotubes for Bone Tissue Engineering," University of Sydney, 2016.

28. D. P. A. Bankoff, "Biomechanical Characteristics of the Bone," Hum. Musculoskelet. Biomech., pp. 61–86, 2012.

29. E. Hamed, Y. Lee, and I. Jasiuk, "Multiscale modeling of elastic properties of cortical bone," in Acta Mechanica, 2010, vol. 213, no. 1–2, pp. 131–154.

30. M. Jassal and S. Ghosh, "Aramid fibres-An overview," Indian J. Fibre Text. Res., vol. 27, no. 3, pp. 290–306, 2002.

31. ho, L. Kuhn-Spearing, and P. Zioupos, "Mechanical properties and the hierarchical structure of bone," Med. Eng. Phys., vol. 20, no. 2, pp. 92–102, 1998.

32. [B. Ji and H. Gao, "Elastic properties of nanocomposite structure of bone," Compos. Sci. Technol., vol. 66, no. 9, pp. 1209–1215, 2006.

33. B. D. Ratner, A. S. Hoffman, F. J. Schoen, and J. E. Lemons, Biomaterials science: an introduction to materials in medicine. 2004.

34. J. Li, W. Tian, H. Yan, L. He, and X. Tuo, "Preparation and performance of aramid nanofiber membrane for separator of lithium ion battery," J. Appl. Polym. Sci., vol. 133, no. 30, 2016.

35. Yang et al., "Dispersions of aramid nanofibers: A new nanoscale building block," ACS Nano, vol. 5, no. 9, pp. 6945–6954, 2011.

36. L. A. Dobrzański, A. Pusz, and A. J. Nowak, "Aramid-silicon laminated materials with special properties – new perspective of its usage," J. Achievemnets Mater. Manuf. Eng., vol. 28, no. 1, pp. 7–14, 2008.

37. C. Nie, Y. Yang, Z. Peng, C. Cheng, L. Ma, and C. Zhao, "Aramid nanofiber as an emerging nanofibrous modifier to enhance ultrafiltration and biological performances of polymeric membranes," J. Memb. Sci., vol. 528, pp. 251–263, 2017.

38. C. Lorandi, "A Smart Solution for Tissue Engineering Applications," University of Trento, 2012.

39. N. Alkhouli et al., "The mechanical properties of human adipose tissues and their relationships to the structure and composition of the extracellular matrix," Am. J. Physiol. Metab., vol. 305, no. 12, pp. E1427–E1435, 2013.

40. D. Lee, H. Zhang, and S. Ryu, "Elastic Modulus Measurement of Hydrogels," in Cellulose-Based Superabsorbent Hydrogels, Springer International Publishing, 2018, pp. 1–21.

41. ISO 10993-5, "A practical guide to ISO 10993-5: Cytotoxicity," Med. Device Diagnostic Ind. Mag., pp. 2–4, 1998.

42. [G. J. López, M. Lehocký, P. Humpolíček, and P. Sáha, "HaCaT Keratinocytes Response on Antimicrobial Atelocollagen Substrates: Extent of Cytotoxicity, Cell Viability and Proliferation," J. Funct. Biomater., vol. 5, no. 2, pp. 43–57, 2014.

43. H. Wan, R. L. Williams, P. J. Doherty, and D. F. Williams, "The cytotoxicity evaluation of Kevlar and silicon carbide by MTT assay," J. Mater. Sci. Mater. Med., vol. 5, no. 6–7, pp. 441–445, 1994.

AUTHORS PROFILE

Nurulhuda Arifin, is a Lecturer in Universiti Kuala Lumpur (UniKL) and pursued her study in doctoral level at School of Mechanical Engineering, Universiti Teknology Malaysia (UTM). Her research is based on fabrication biomaterial by using DLP 3D printing technoloqy for application of 3D tissue engineering scaffold. Her research interest involved several areas include materials engineering, biomaterial, tissue engineering, additive manufacturing, machining and 3D printing.

Professor Izman Sudin, is currently attached with the School of Mechanical Engineering, Faculty of Engineering at the Universiti Teknologi Malaysia. His research interests involved several areas include precision machining of hard and brittle materials, surface treatment and coating, corrosion, implant materials, additive manufacturing and functional graphene..

Nor Hasrul Akhmal Ngadiman, is a Senior Lecturer in the Department of Materials, Manufacturing and Industrial Engineering,School of Mechanical Engineering (SME), Faculty of Engineering, Universiti Teknologi Malaysia, Johor Bahru, Johor, Malaysia. He is also a member of Adavnce Manufacturing Research Group and Frontier Materials Research Alliance. His research interests are in the areas of biomaterials, nanomaterials, additive/advanced manufacturing process, tissue engineering, quality improvement, safety, and ergonomi